

# Machine learning method for single trajectory characterization

Gorka Muñoz-Gil,<sup>1</sup> Miguel Angel Garcia-March,<sup>1</sup> Carlo Manzo,<sup>2</sup> José D. Martín-Guerrero,<sup>3</sup> and Maciej Lewenstein<sup>1,4</sup>

<sup>1</sup>*ICFO – Institut de Ciències Fotòniques, The Barcelona Institute of Science and Technology, 08860 Castelldefels (Barcelona), Spain*

<sup>2</sup>*Facultat de Ciències i Tecnologia, Universitat de Vic – Universitat Central de Catalunya (UVic-UCC), C. de la Laura,13, 08500 Vic, Spain*

<sup>3</sup>*Universitat de València – IDAL, Department of Electronic Engineering, ETSE-UV, Avda. Universitat, s/n 46100 Burjassot (Valencia), Spain*

<sup>4</sup>*ICREA, Lluís Companys 23, E-08010 Barcelona, Spain*

In order to study transport in complex environments, it is extremely important to determine the physical mechanism underlying diffusion, and precisely characterize its nature and parameters. Often, this task is strongly impacted by data consisting of trajectories with short length and limited localization precision. In this paper, we propose a machine learning method based on a random forest architecture, which is able to associate even very short trajectories to the underlying diffusion mechanism with a high accuracy. In addition, the method is able to classify the motion according to normal or anomalous diffusion, and determine its anomalous exponent with a small error. The method provides highly accurate outputs even when working with very short trajectories and in the presence of experimental noise. We further demonstrate the application of transfer learning to experimental and simulated data not included in the training/testing dataset. This allows for a full, high-accuracy characterization of experimental trajectories without the need of any prior information.

A range of experimental techniques, embracing a wide number of fields of research, relies on the tracking of the position of single particles over time. The thorough quantification and classification of the collected trajectories allows to learn valuable information about the parameters and the type of motion performed by the tracker, thus providing insight about the environment where diffusion takes place [1]. Commonly, the trajectories are analyzed by quantifying the (time-averaged) mean square displacement (MSD) versus the time lag  $T_{\text{lag}}$  [2]:

$$\overline{\delta^2(T_{\text{lag}})} = \frac{1}{t - T_{\text{lag}}} \int_0^{t-T_{\text{lag}}} [x(t' + T_{\text{lag}}) - x(t')]^2 dt'. \quad (1)$$

While a Brownian walker in a homogeneous environment shows a linear increase of the MSD, other types of transport show anomalous behaviors, characterized by an asymptotic nonlinear scaling of the MSD curve  $\overline{\delta^2} \sim T_{\text{lag}}^\alpha$ .

The observation of these anomalous behaviors is widespread in biology and soft matter, due to the complexity of the environment and the presence of interactions [1]. Therefore, the exponent  $\alpha$  of the MSD is widely used to determine whether the type of diffusion is normal or anomalous. Several methods have been proposed to accurately estimate this exponent [3, 4] in the presence of experimental limitations, such as thermal noise and the finite length of the trajectory. The emergence of anomalous behavior has also been widely studied from the theoretical point of view and conceptually-different models have been proposed [2]. However, the fact that models with different physical properties can produce the same MSD exponent, strongly limits the unambiguous determination of the underlying dynamics, based only on the evaluation of the MSD. In order to solve this ambiguity, a large effort has been made to classify experimental data showing anomalous transport. As an ex-

ample, the use of alternative estimators [5, 6] has been proposed to determine whether the pioneering results of Golding and Cox [7] were arising from a continuous-time random walk (CTRW) [8] or fractional Brownian motion (FBM) [9]. This search for a better classification between CTRW and FBM often relied in the determination of the (non)ergodicity of the data [6, 10–12], i.e. the nonequivalence of time and ensemble averages of the MSD, since CTRW is consistent with weak ergodicity breaking [13]. In the nonergodic case,  $\overline{\delta^2(T_{\text{lag}})}$  remains random even in the long measurement times, i.e., the diffusion coefficients are irreproducible but the distribution of the MSD is universal [14]. Evidence of nonergodic behavior has also been experimentally observed in biology as a consequence of diffusion in heterogeneous environment [15–18] and have boosted the proposal of new theoretical frameworks consistent with these features [19, 20]. For nonergodic models, the determination of the anomalous exponent cannot be performed at the single trajectory level and requires the calculation of the MSD over an ensemble of trajectories [2].

In this scenario, determining whether a single trajectory displays normal or anomalous behavior, characterizing its MSD scaling exponent, and associating the motion to its underlying physical mechanism are elements of paramount importance to provide a detailed picture of a variety of phenomena. Recent works in this direction have focused on classification schemes based on Power Spectral Density [21], or Bayesian approaches [22, 23]. Surprisingly, in spite of the fast rise of machine learning (ML) methods, little efforts have been made in this sense to classify single trajectories. Moreover, they have been mainly directed to qualitatively discriminate among confined, anomalous, normal or directed motion [24, 25]. However, these approaches show limitations when at-

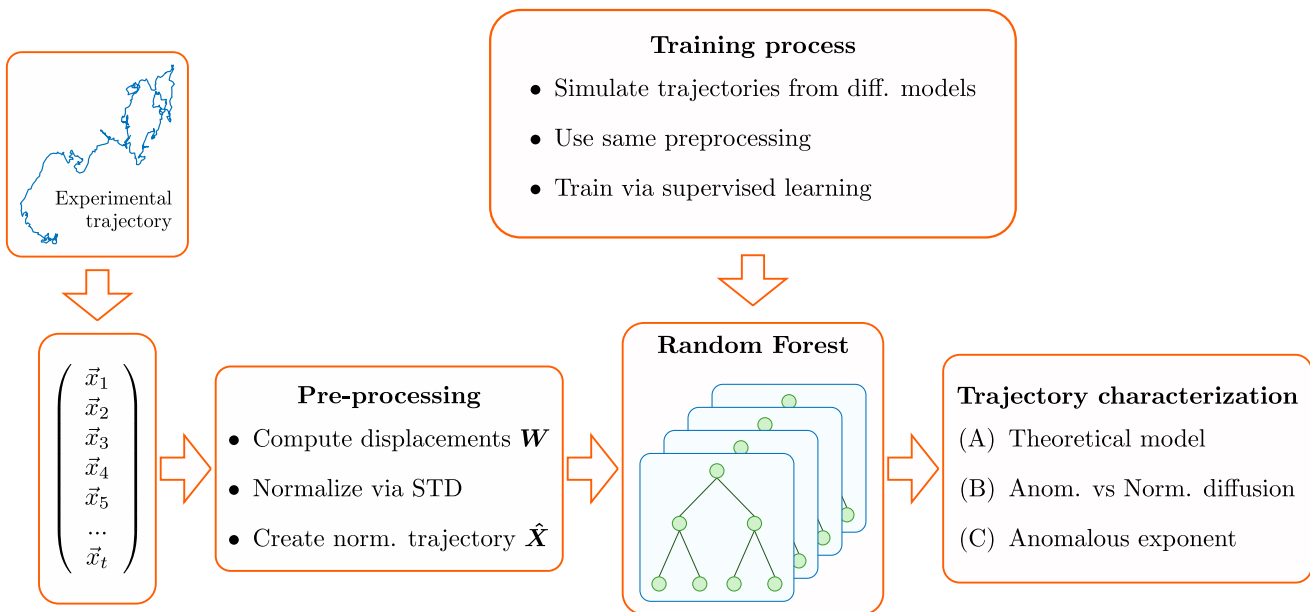


FIG. 1. **Schematic of the method:** when classifying a new experimental trajectory, we first transform the trajectory to a vector of positions in given times. Then, we use the preprocessing described in Section I. Finally, the trajectory is characterized by a RF, trained previously with simulated trajectories. In this work, we show how to extract three characteristics of the trajectory via ML: (A) the closest theoretical model from the ones contained in the training dataset, (B) if the trajectory is normal or anomalous diffusing, and (C) the anomalous exponent  $\alpha$ .

tempting to determine the anomalous exponent for non-ergodic trajectories.

This paper presents a ML algorithm based on the Random Forest (RF) architecture that efficiently and robustly classifies single trajectories at three different levels: obtaining the discrimination among several diffusion models, the classification between normal and anomalous diffusion, and the estimation of the exponent that characterizes the anomalous diffusion. The algorithm allows to accurately tackle these challenging problems even when dealing with short and noisy trajectories.

## I. CLASSIFICATION METHOD

In this section, we will review the main parts of the classification algorithm, consisting in: the ML algorithm that takes the form of a RF architecture; the simulated dataset; and the preprocessing applied to the dataset before being analyzed by the RF. Figure 1 shows a schematic representation of the pipeline.

*Random Forest* RF is an architecture based on Decision Trees (DTs). DT is an efficient non-parametric method widely used for classification and regression problems [26]. The basic idea consists in producing recursive binary splits of the input space, so that the samples with the same label are grouped together. The criterion to produce the splits is based on a homogeneity measure (usually, the information entropy) of the target variable within each of the obtained groups. Once a DT is ob-

tained, the output for unseen samples is computed just passing them through the nodes of the tree, where a decision is made with respect to which direction to take. Finally, a terminal tree node is reached, where the output is obtained. A RF is a tree-based ensemble method, which builds several DT models independently and then computes a final prediction by combining the outputs of the different individual trees [27]. In classification trees, the ones used in this work, a majority voting scheme is usually applied. In particular, the ensemble is produced with single trees built from samples drawn randomly with replacement (bootstrap) from the training set. An additional randomness is added when splitting a tree node because the split is chosen among a random subset of the input variables, selected in this case without replacement, instead of the greedy approach of considering all the input variables. Due to this randomization, the bias of the ensemble is slightly higher than that of a single tree, but the variance is decreased and the model is more robust to variations in the dataset. As shown in a thorough comparison study [28], besides clearly outperforming single DTs in complex problems, RF is also the most suitable choice in many different classification problems.

*Training and testing datasets* The training dataset is built out of numerical simulations of trajectories from various kinds of theoretical models. As a natural choice, we included three of the best-known and used models that can give rise to anomalous diffusion: CTRW [8], FBM [9] and Lévy walks (LW) [29]. In addition, we included trajectories from the annealed transient time

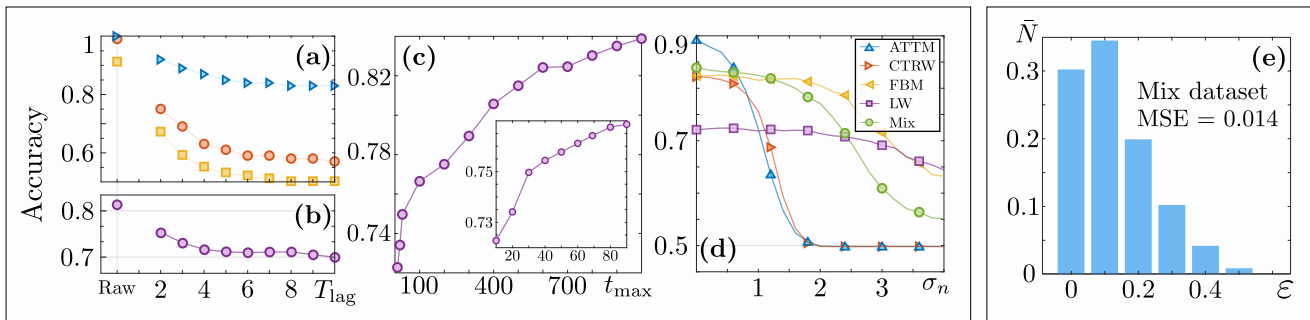


FIG. 2. **Benchmarking the RF algorithm:** (a) Accuracy of the RF when discriminating among models. Blue triangles = CTRW vs FBM, Red circles= CTRW, LW, FBM, ATTMM, and Yellow squares= CTRW vs ATTMM. (b) Accuracy of the RF trained to classify between normal and anomalous trajectories. The dataset contains trajectories coming from the models CTRW, FBM, LW and PM. (c) Accuracy of the RF as a function of the length  $t_{\text{max}}$  of the trajectory. Inset shows values for smaller values of  $t_{\text{max}}$ . (d) Accuracy of a RF trained on a dataset made of certain models, and then asked to classify trajectory of such models with normal noise given by Eq. (3). (e) Anomalous exponent prediction. Y-axis is percentage of trajectories  $\bar{N}$  with given error  $\epsilon$  when predicting the value of  $\alpha$ . We consider a range of  $\alpha \in [0.5, 1]$  with  $\Delta\alpha = 0.1$ .

model (ATTM) [19]. In the ATTM, a diffuser performs a random walk but stochastically changes the diffusion coefficient at random times. Both the diffusion coefficient and the time at which the diffusivity changes are drawn from distributions with power law behavior [19]. Its time-averaged MSD shows a linear scaling, but the model has a regime in which it displays weak ergodicity breaking. The ATTM has been shown to reproduce the features observed for the diffusion of a cell membrane receptor [18], one of the experimental datasets analyzed.

*Preprocessing* Our aim is to design a method able to accurately classify heterogeneous trajectories. In particular, the method should work equally for diffusion taking place at different spatio-temporal scales. It is thus fundamental to design a preprocessing step that properly rescale the data. For this reason, we implemented the following procedure:

1. We use one of the models above to simulate the trajectory of a particle during  $t_{\text{max}}$  time steps. The result is a vector of positions,  $\mathbf{X} = (\mathbf{x}_1, \mathbf{x}_2, \dots, \mathbf{x}_{t_{\text{max}}})$ .
2. This vector is transformed into a vector of distances traveled in an interval of time  $T_{\text{lag}}$ , i.e.,  $\mathbf{W} = (\Delta\mathbf{x}_1, \Delta\mathbf{x}_2, \dots, \Delta\mathbf{x}_{J-1})$ , where  $J = t_{\text{max}}/T_{\text{lag}}$ . We define  $\Delta\mathbf{x}_i$  as

$$\Delta\mathbf{x}_i = |\mathbf{x}_{iT_{\text{lag}}} - \mathbf{x}_{(i+1)T_{\text{lag}}}|. \quad (2)$$

3. To normalize the data, we divide  $\mathbf{W}$  by its standard deviation (STD) to get a new vector  $\hat{\mathbf{W}}$ .
4. Then, we do a cumulative sum of  $\hat{\mathbf{W}}$  to construct a normalized trajectory  $\hat{\mathbf{X}}$ .

The same preprocessing was also applied to the simulated and experimental trajectories used in Section III.

## II. TRAJECTORY CHARACTERIZATION AS A CLASSIFICATION PROBLEM

We will use our method to characterize single trajectories according to three different classification schemes: (A) discrimination among diffusion models; (B) classification as normal or anomalous diffusion; and (C) prediction of the anomalous exponent  $\alpha$ . For each of these problems, we created a dataset of  $3 \cdot 10^4$  trajectories with  $t_{\text{max}} = 10^3$ , divided into a training and test set with ratio 0.8/0.2 respectively. The different classes considered in each problem have an equal number of trajectories, hence allowing us to use the accuracy as a measure of the goodness of the RF. For technical details and an example on the implementation, we refer the reader to Ref. [30].

*A. Discrimination among diffusion models* In order to predict the diffusion model underlying a certain trajectory, we construct a RF whose input is the normalized trajectory  $\hat{\mathbf{X}}$ , and the output is a number between 0 and  $N - 1$  corresponding to the different models, with  $N$  the total number of models used in the training. Figure 2(a) shows the accuracy of the RF. Each line corresponds to a training dataset built out of different models. In the absence of data preprocessing (point marked as 'Raw' in the x-axis), the RF shows large accuracy. However, the accuracy drops significantly as  $T_{\text{lag}}$  increases, likely as a consequence of the removal of microscopical properties of the model, such as short-time correlations, hence preventing the RF from learning important features of them. This might lead to the conclusion that the filtering introduced by the preprocessing steps only limits the time resolution. This is obviously true for simulated data, obtained at the same scale, for which preprocessing is unnecessary. However, when dealing with experimental data of unknown spatiotemporal scale, such a preprocessing is of fundamental importance to be able to apply the same architecture and training dataset, in spite of the little loss of performance.

In addition, the accuracy heavily depends on similarities among the models to be discriminated. For example, the accuracy obtained with a RF trained only with trajectories reproducing conceptually different models such as FBM and CTRW (triangular markers in Fig. 2(a)) is higher than the one obtained when including in the training models with similar characteristics, such as the CTRW and the ATTMM, independently of  $T_{\text{lag}}$  (red circles and yellow squares in Fig. 2(a)).

*B. Normal vs Anomalous diffusion* To discriminate between normal or anomalous diffusion, we rely on a RF whose output is 0 for normal diffusing trajectories and 1 for anomalous diffusion. The results of such classification problem are shown in Fig. 2 (b). We consider a dataset of trajectories with  $\alpha \in [0.2, 2]$ , thus covering both sub and superdiffusion. Also in this case, increasing  $T_{\text{lag}}$  impacts the accuracy of the RF. However, the loss of accuracy is not as pronounced as in the previous problem.

A remarkable feature of our method is the possibility to correctly classify very short trajectories. In Fig 2(c) we show the accuracy of the RF when classifying anomalous *vs.* normal trajectories as a function of their length  $t_{\text{max}}$ . Although we observe an expected decrease of performance for short trajectories, we obtain an astonishing accuracy of 0.72 when classifying trajectories of only 10 points.

Finally, we remark that the accuracy of the classification of an anomalous trajectory depends heavily on the value of the exponent  $\alpha$  value. As expected, the further away from 1, the higher the accuracy. Consequently, even if the classifier is robust with respect to little variations of the exponent, trajectories corresponding to values of  $\alpha$  close to 1 are classified as normal diffusion. This produces a loss of accuracy for subdiffusive trajectories with exponent  $\alpha \sim 1$ . We will further comment on this problem and possible solutions in Section III.

Experimental trajectories have a limited localization precision that results into Gaussian noise. Therefore, it is important to test the robustness to noise of the RF. For this, we trained the RF with trajectories simulated as described before and then try to classify trajectories belonging to the same processes, but which positions  $\mathbf{X}$  were corrupted with noise to obtain the dataset  $\mathbf{X}^{(n)}$

$$\mathbf{x}_i^{(n)} = \mathbf{x}_i + \mu_i(\mu, \sigma_n), \quad (3)$$

where  $\mu_i(\mu, \sigma_n)$  is a random number retrieved from a Normal distribution with mean  $\mu = 0$  and variance  $\sigma_n$ . The results obtained for training with each specific model or when all are considered simultaneously are represented in Fig. 2(d). The RF shows a great robustness against noise. For  $\sigma_n < 1$ , the accuracy appears almost unaffected. When increasing  $\sigma_n$ , we see that the accuracy drops in a model-dependent manner. The drop is more pronounced when training only with CTRW or ATTMM, smaller when training with FBM and much smaller when training with LWs. Similar to what pointed out before for the dependence on  $T_{\text{lag}}$ , this also seems to highlight that

short-time features of CTRW and ATTMM play a major role when classifying these kind of trajectories.

*C. Anomalous exponent estimation* The third classification problem requires to construct a multiclass problem, in which the output of the RF is the value of the anomalous exponent  $\alpha$ . To follow a classification paradigm as in the rest of the paper, a finite number of outputs was considered, thus the values of  $\alpha$  were discretized in steps of  $\Delta\alpha$ . Obviously, the smaller  $\Delta\alpha$ , the larger the number of classes, hence the difficulty of the problem increases.

To characterize the performance of the method, we calculate the prediction error  $\varepsilon$  of a trajectory as the absolute distance between the predicted exponent and the ground truth value. The percentage of trajectories  $\bar{N}(\varepsilon)$  with a given error  $\varepsilon$  is represented in the bar plot of Fig. 2(e) for a subdiffusive dataset including trajectories obtained from FBM, CTRW and ATTMM. We calculated a mean squared error of the prediction of the anomalous exponent of 0.014, corresponding to determining the exponent of  $\sim 65\%$  of the trajectories within 0.1 from the true value.

### III. TRANSFER LEARNING IN SIMULATED AND EXPERIMENTAL DATA

To further show the advantages of our ML algorithm, we applied it to three sets of trajectories different from those included in the training/testing dataset. This is often referred as transfer learning, as certain architecture is trained in one setting and then applied to a different one. For this, we will consider three datasets:

- (i) Simulated data coming from a recently presented model [31], describing the movement of a diffuser in a network of compartments of random size and random permeability, both drawn from universal distributions. This model shares the same subordination as the quenched trap model, i.e. a CTRW with power-law distributed trapping times and recapitulates the complexity and heterogeneity found in some biological environments. This choice allows to test the algorithm over a conceptually different model with respect to the training dataset, while having the advantage of tuning the value of anomalous exponents.
- (ii) Experiment 1, reporting the motion of individual mRNA molecules inside live bacterial cells [7]. The MSD shows anomalous diffusion with  $\alpha \sim 0.7$ ; this behavior has been associated to FBM [5, 32].
- (iii) Experiment 2, corresponding to a set of trajectories obtained for the diffusion of a membrane receptor in living cells [18]. Although the time-averaged MSD shows a nearly linear behavior, the data present features of ergodicity breaking due to changes of diffusivity [33] and have been associated to the ATTMM model.

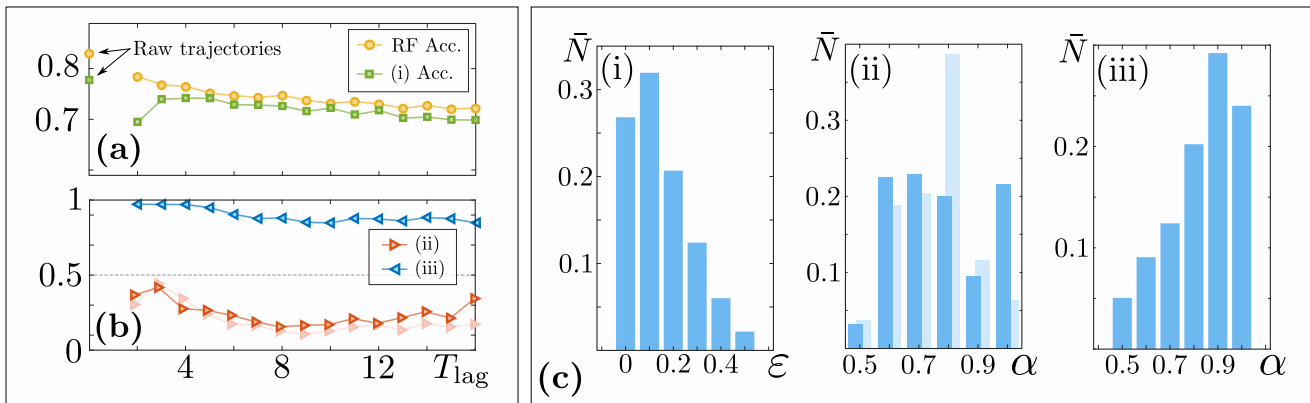


FIG. 3. **Transfer learning: characterizing unknown trajectories.** (a) Anomalous *vs* normal classification accuracy for the simulated dataset (i). We also present the accuracy of the model and show that both behave in a similar way. (b) Anomalous *vs* normal classification for the experimental datasets (ii) and (iii). The y-axis is the percentage of trajectories classified as normal diffusing. The close to zero, the more trajectories have been classified as anomalous. For dataset (ii), we present results for two different training sets: one including all subdiffusive models considered in Section I (bolded) and another including only FBM trajectories (shadowed). (c) Anomalous exponent prediction. For dataset (i), we plot the percentage of trajectories  $\bar{N}$  where the predicted value of  $\alpha$  has an absolute error  $\varepsilon$ . As it is a simulated dataset, exponents from 0.2 to 1 are considered. For datasets (ii) and (iii), we present the percentage of trajectories predicted to have an anomalous exponent  $\alpha$ . For dataset (iii), again, we present results for the two training datasets discussed previously: dark blue for the mixed dataset and light blue for the FBM dataset.

Following the scheme presented in Fig. 1, first we train the RF with simulated trajectories obtained with different theoretical frameworks. It should be noted that for this section, since we deal with trajectories that do not show superdiffusive behavior, we do not include the LW process in the training dataset.

*Results* Following the same structure of the previous section, we start by discriminating the diffusion model that can be associated to datasets (i)-(iii). The results are reported in Table I, showing a high rate of correct classification for the dataset (i). For the experimental data in datasets (ii) and (iii), we do not dispose of ground truth values, thus we compare our results with those of previous analysis, performed with alternative methods. For the trajectories of Experiment 1, we found that the algorithm largely assign them to the FBM, in strong agreement with previously reported results based on the concept of variation [5]. The data of Experiment 2 are mainly assigned to the ATTM model. This model was shown to reproduce features observed in these data, such as subdiffusion and weak ergodicity breaking [18]. Moreover, a little fraction of trajectories are classified as CTRW. As previously mentioned, CTRW and ATTM share similar features, increasing the difficulty in discriminating between them. This appears to be the main source of error in the results.

Next, we focus on the normal *vs.* anomalous diffusion problem. For the simulated dataset (i) (see Fig. 3(a)), the accuracy follows closely the RF accuracy, with a small offset due to the error introduced by transfer learning. We observe a small drop in accuracy for  $T_{lag} = 2$ , probably

Dataset	Predicted Model		
	CTRW	FBM	ATTM
(i) Compartments model	<b>89.2%</b>	0	10.7%
(ii) Experiment 1	4.5%	<b>86.6%</b>	8.9%
(iii) Experiment 2	16.4%	33.2%	<b>50.4%</b>

TABLE I. Process discrimination for the datasets considered in section III. Shown is the percentage of trajectories classified as associated to each model. The results for (i) were done with  $T_{lag} = 0$  and for datasets (ii) and (iii) with  $T_{lag} = 2$ .

due to the spatial properties of the model. The results of the experimental datasets are presented in Fig. 3(b), where we plot the percentage of trajectories classified as normal diffusing. For the dataset (ii) the RF predicts anomalous diffusion for  $\sim 30 - 40\%$  of the trajectories, consistently with the observation reported in the original work [7]. For the dataset (iii), the RF classifies as anomalous only a small fraction of trajectory. In this case, the occurrence of subdiffusion was inferred from ensemble analysis of the MSD. Due to nonergodicity, single trajectories showed a nearly linear MSD. In addition, the anomalous exponent observed in this case had a value closer to 1, thus setting us in the region where this problem shows lower accuracy.

For this kind of classification, the performance of the method can be further improved by taking advantage of the results of the model discrimination discussed above and shown in Table I. In fact, when the latter classification indicates that most of the trajectories follow a

specific diffusive model, one can train the algorithm with a dataset composed only of trajectories simulated with that model. As an example, we applied this rationale to the trajectories of Experiment 1 (ii). As shown in Fig. 3(b), this produces the RF to predict a higher number of subdiffusive trajectories (shadow red) with respect to the original prediction (red).

To obtain further insights on the study of the diffusion, we used the RF to characterize the anomalous exponents. For the first dataset (i), based on simulations, we generated trajectories having a broad range of subdiffusive trajectories, i.e.  $\alpha \in [0.2, 1]$  and evaluated the error as the absolute value of the difference between the actual and predicted  $\alpha$ . The results are reported in the histogram of Fig. 3(c) (i) and display a distribution similar to the one obtained for the training/testing data. Thus, we run this type of classification on the experimental data. For the two datasets, in Fig. 3(c) (ii)-(iii) we report the values obtained for the anomalous exponent  $\alpha$ . The histogram of the  $\alpha$  obtained for the trajectories of Experiment I (light blue) shows mainly subdiffusive values, peaked in the range  $0.6 - 0.8$ . This is in good agreement with the original paper [7], where  $\alpha$  was estimated by means of two different approaches as 0.7 and 0.77. However, the method also classifies a percentage of the trajectories as having  $\alpha = 1$ , similarly as what observed for the normal *vs.* anomalous problem. As also noted above, this estimation can be improved by the use of a training performed with a specific model. This kind of training produces exponent values in the same range, but largely reduce the fraction of those associated to  $\alpha = 1$ , as shown in Fig. 3(c) (ii) (light blue).

Last, in Fig. 3(c) (iii) we plot the distribution of exponents obtained for the Experiment 2. The subdiffusive values show a large number of occurrences in the  $0.8 - 0.9$  range, compatible with the exponent 0.84 calculated in previous studies [18]. Noteworthy, due to the nonergodic nature of the data,  $\alpha$  could only be calculated from the ensemble-averaged MSD, whereas the RF is able to determine this exponent from single trajectories. In addition, it is interesting to note that in this case, the percentage of trajectories classified as  $\alpha = 1$  ( $\sim 20\%$ ) is much smaller than those ( $\sim 90\%$ ) classified as normal with the previous classification (the normal *vs.* anomalous problem). The exponent classification can thus also be used as a way to improve the performance of this classification for anomalous exponent close to 1.

#### IV. CONCLUSIONS

We presented a machine learning method, based on a Random Forest architecture, which is capable to consider a single trajectory and to determine the theoretical

model that describes it at best. The same method is used to classify the motion as normal or anomalous, and predict its anomalous exponent with high accuracy. The method does not need any prior information over the nature of the system from which the trajectory is obtained. It acts as a blackbox, which we train with a dataset of simulated trajectories, and then it is used to characterize the trajectory of interest. In particular, its spatial scale is not of any relevance, as we devised a preprocessing strategy which rescales trajectories to obtain comparable estimators from very different systems. The method requires a minimal amount of information. First, because it performs extremely well even with surprisingly short trajectories. Second, because it is robust with respect to the presence of a large amount of thermal noise, and can thus be applied even with low localization precision. We showcase the suitability of our method by applying it to two experimental datasets by means of transfer learning. Overall, this method can be of large application to characterize experiments from several research areas. In contrast to other methods, it can determine the type of diffusion and the anomalous exponent also for nonergodic models, without the need of performing ensemble averages. Further development can include the use of regression RF for the prediction of the exact value of the anomalous exponent. Moreover, recent works show how other ML architectures, such as convolutional neural networks, are also capable of doing single trajectory characterization [25]. The development of these methods and of other deep learning architectures may help to avoid the preprocessing procedure and could lead to increase the accuracy on the problems described in this work.

#### ACKNOWLEDGMENTS

This work has been funded by the Spanish Ministry MINECO (National Plan15 Grant: FISICATEAMO No. FIS2016-79508-P, SEVERO OCHOA No. SEV-2015-0522, FPI), European Social Fund, Fundació Cellex, Generalitat de Catalunya (AGAUR Grant No. 2017 SGR 1341 and CERCA/Program), ERC AdG OSYRIS, EU FETPRO QUIC, and the National Science Centre, Poland-Symfonia Grant No. 2016/20/W/ST4/00314. C.M. acknowledges funding from the Spanish Ministry of Economy and Competitiveness and the European Social Fund through the Ramón y Cajal program 2015 (RYC-2015-17896) and the BFU2017-85693-R and from the Generalitat de Catalunya (AGAUR Grant No. 2017SGR940). G.M. acknowledges financial support from Fundaci Social La Caixa. We gratefully acknowledge the support of NVIDIA Corporation with the donation of the Titan Xp GPU.

---

[1] C. Manzo and M. F. Garcia-Parajo, “A review of progress in single particle tracking: from methods to biophysical

insights,” *Rep. Prog. Phys.*, vol. 78, 12, 124601, 2015.

- [2] R. Metzler, J.-h. Jeon, A. G. Cherstvy, and E. Barkai, “Anomalous diffusion models and their properties: non-stationarity, non-ergodicity, and ageing at the centenary of single particle tracking,” *Phys. Chem. Chem. Phys.*, vol. 16, pp. 24128–24164, 2014.
- [3] E. Kepten, I. Bronshtein, and Y. Garini, “Improved estimation of anomalous diffusion exponents in single-particle tracking experiments,” *Phys. Rev. E*, vol. 87, p. 052713, May 2013.
- [4] K. Burnecki, E. Kepten, Y. Garini, G. Sikora, and A. Weron, “Estimating the anomalous diffusion exponent for single particle tracking data with measurement errors - An alternative approach,” *Scientific Reports*, vol. 5, no. May, p. 11306, 2015.
- [5] M. Magdziarz, A. Weron, and K. Burnecki, “Fractional Brownian Motion Versus the Continuous-Time Random Walk: A Simple Test for Subdiffusive Dynamics,” *Physical Review Letters*, vol. 103, p. 180602, oct 2009.
- [6] M. Magdziarz and A. Weron, “Anomalous diffusion: Testing ergodicity breaking in experimental data,” *Physical Review E*, vol. 84, p. 051138, nov 2011.
- [7] I. Golding and E. C. Cox, “Physical nature of bacterial cytoplasm,” *Phys. Rev. Lett.*, vol. 96, p. 098102, Mar 2006.
- [8] J. Klafter and I. M. Sokolov, *First Steps in Random Walks*. Oxford University Press, 2011.
- [9] B. Mandelbrot and J. Van Ness, “Fractional brownian motions, fractional noises and applications,” *SIAM Review*, vol. 10, no. 4, pp. 422–437, 1968.
- [10] W. Deng and E. Barkai, “Ergodic properties of fractional Brownian-Langevin motion,” *Physical Review E - Statistical, Nonlinear, and Soft Matter Physics*, vol. 79, no. 1, pp. 1–7, 2009.
- [11] Y. Meroz and I. M. Sokolov, “A Toolbox for Determining Subdiffusive Mechanisms,” *Physics Reports*, vol. 573, pp. 1–29, 2015.
- [12] Y. Lanoiselée and D. S. Grebenkov, “Revealing nonergodic dynamics in living cells from a single particle trajectory,” *Physical Review E*, vol. 93, no. 5, p. 052146, 2016.
- [13] J.-P. Bouchaud, “Weak ergodicity breaking and aging in disordered systems,” *Journal de Physique I*, vol. 2, pp. 1705–1713, 1992.
- [14] T. Akimoto and E. Yamamoto, “Distributional behavior of diffusion coefficients obtained by single trajectories in annealed transit time model,” *Journal of Statistical Mechanics: Theory and Experiment*, vol. 2016, p. 123201, dec 2016.
- [15] J.-H. Jeon, V. Tejedor, S. Burov, E. Barkai, C. Selhuber-Unkel, K. Berg-Sørensen, L. Oddershede, and R. Metzler, “In Vivo Anomalous Diffusion and Weak Ergodicity Breaking of Lipid Granules,” *Physical Review Letters*, vol. 106, p. 048103, jan 2011.
- [16] A. V. Weigel, B. Simon, M. M. Tamkun, and D. Krapf, “Ergodic and nonergodic processes coexist in the plasma membrane as observed by single-molecule tracking,” *Proceedings of the National Academy of Sciences of the United States of America*, vol. 108, pp. 6438–43, apr 2011.
- [17] S. M. A. Tabei, S. Burov, H. Y. Kim, A. Kuznetsov, T. Huynh, J. Jureller, L. H. Philipson, A. R. Dinner, and N. F. Scherer, “Intracellular transport of insulin granules is a subordinated random walk,” *Proceedings of the National Academy of Sciences of the United States of America*, vol. 110, pp. 4911–6, mar 2013.
- [18] C. Manzo, J. a. Torreno-Pina, P. Massignan, G. J. Lapeyre, M. Lewenstein, and M. F. Garcia Parajo, “Weak Ergodicity Breaking of Receptor Motion in Living Cells Stemming from Random Diffusivity,” *Physical Review X*, vol. 5, p. 011021, feb 2015.
- [19] P. Massignan, C. Manzo, J. A. Torreno-Pina, M. F. García-Parajo, M. Lewenstein, and G. J. Lapeyre, “Non-ergodic subdiffusion from brownian motion in an inhomogeneous medium,” *Physical Review Letters*, vol. 112, no. 3, pp. 1–5, 2014.
- [20] M. V. Chubynsky and G. W. Slater, “Diffusing Diffusivity: A Model for Anomalous, yet Brownian, Diffusion,” *Physical Review Letters*, vol. 113, p. 098302, aug 2014.
- [21] D. Krapf, E. Marinari, R. Metzler, G. Oshanin, X. Xu, and A. Squarcini, “Power spectral density of a single brownian trajectory: what one can and cannot learn from it,” *New Journal of Physics*, vol. 20, p. 023029, feb 2018.
- [22] K. Hinsén and G. R. Kneller, “Communication: A multiscale Bayesian inference approach to analyzing subdiffusion in particle trajectories,” *Journal of Chemical Physics*, vol. 145, no. 15, pp. 0–5, 2016.
- [23] S. Thapa, M. A. Lomholt, J. Krog, A. G. Cherstvy, and R. Metzler, “Bayesian analysis of single-particle tracking data using the nested-sampling algorithm: maximum-likelihood model selection applied to stochastic-diffusivity data,” *Phys. Chem. Chem. Phys.*, vol. 20, pp. 29018–29037, 2018.
- [24] P. Dosset, P. Rassam, L. Fernandez, C. Espenel, E. Rubinstein, E. Margeat, and P.-E. Milhiet, “Automatic detection of diffusion modes within biological membranes using back-propagation neural network,” *BMC bioinformatics*, vol. 17, no. 1, p. 197, 2016.
- [25] P. Kowalek, H. Loch-Olszewska, and J. Szwański, “Classification of diffusion modes in single particle tracking data: feature based vs. deep learning approach,” *arXiv preprint arXiv:1902.07942*, 2019.
- [26] L. Breiman, J. H. Friedman, R. A. Olshen, and C. J. Stone, *Classification and regression trees*. Belmont, California, USA: Wadsworth Publishing Company, 1984.
- [27] L. Breiman, “Random forests,” *Machine Learning*, vol. 45, no. 1, pp. 5–32, 2001.
- [28] M. Fernández-Delgado, E. Cernadas, S. Barro, and D. Amorim, “Do we need hundreds of classifiers to solve real world classification problems?,” *Journal of Machine Learning Research*, vol. 15, pp. 3133–3181, 2014.
- [29] V. Ziburdaev, S. Denisov, and J. Klafter, “Lévy walks,” *Rev. Mod. Phys.*, vol. 87, pp. 483–530, Jun 2015.
- [30] G. Muñoz Gil, “RF-single-trajectory-characterization,” <https://github.com/gorkamunoz/RF-Single-Trajectory-Characterization>, 2019.
- [31] G. Muñoz Gil, M. A. García-March, C. Manzo, A. Celi, and M. Lewenstein, “Diffusion through a network of compartments separated by partially-transmitting boundaries,” *Frontiers in Physics*, feb 2019.
- [32] D. Molina-García, T. M. Pham, P. Paradisi, C. Manzo, and G. Pagnini, “Fractional kinetics emerging from ergodicity breaking in random media,” *Physical Review E*, vol. 94, p. 052147, 2016.
- [33] M. Balcerk, H. Loch-Olszewska, J. A. Torreno-Pina, M. F. Garcia-Parajo, A. Weron, C. Manzo, and K. Burnecki, “Inhomogeneous membrane receptor diffusion explained by a fractional heteroscedastic time series model,” *Phys. Chem. Chem. Phys.*, vol. 21, pp. 3114–3121, 2019.